Blazed grating fabrication through gray-scale X-ray lithography

Pantazis Mouroulis, Frank T. Hartley, Daniel W. Wilson, Victor E. White

Jet Propulsion Laboratory, California Institute of Technology, Pasadena, CA 91109, USA
pantazis.mouroulis@jpl.masa.gov, frank.t.hartley@jpl.nasa.gov, daniel.w.wilson@jpl.nasa.gov, victor.e.white@jpl.nasa.gov

Aidan Shori, Steven Nguyen, Min Zhang, Martin Feldman

Department of Electrical and Computer Engineering, Louisiana State University, Baton Rouge, LA 70803, USA
ashori@sol.ece.lsu.edu, nguyen@myriadcomputers.com, mzhang@lsu.edu, feldman@ee.lsu.edu

Abstract: Blazed gratings have been fabricated using gray-scale X-ray lithography. The gratings have high efficiency, low parasitic light, and high groove quality. The fabrication technique and resist characterization are described. The gratings can be generated over a considerable range of distances from the X-ray mask, thus demonstrating the ability to write gratings on a substrate of effectively arbitrary shape.

OCIS codes: (050.1950) Diffraction gratings, (220.3740) Lithography

References and links

1. L. Mertz, "Concentric spectrographs," Appl. Opt. **16**, 3122-3124 (1977)
2. D. R. Lobb, "Theory of concentric designs for grating spectrometers," Appl. Opt. **33**, 2648-2658 (1994)
3. D. Kwo, G. Lawrence, and M. Chrisp, "Design of a grating spectrometer from a 1:1 Offner mirror system," SPIE Proc. **818**, 275-279 (1987)
4. P. Mouroulis and M. McKerns, "Pushbroom imaging spectrometer with high spectroscopic data fidelity: experimental demonstration," Opt. Eng. **39**, 808-816 (2000)
5. P. Mouroulis, R. O. Green, and T. G. Chrien, "Design of pushbroom imaging spectrometers for optimum recovery of spectroscopic and spatial information," Appl. Opt. **39**, 2210-2220 (2000)
6. F. Reininger, M. Dami, R. Paolinetti, S. Pieri and S. Falugiani, "Visible infrared mapping spectrometer visible channel (VIMS-V)," in *Instrumentation in Astronomy Viii*, Proc. SPIE **2198**, 239-250 (1994)
7. M. A. Folkman, J. Pearlman, L. B. Liao, and P. J. Jarecke, "EO1/Hyperion hyperspectral imager design, development, characterization and calibration," in *Hyperspectral Remote Sensing of the Land and Atmosphere*, W. L. Smith and Y. Yasuoka Eds., SPIE Proc. **4151**, 40-51 (2001)
8. C. O. Davies, J. Bowles, R. A. Leathers, D. Korwan, T. V. Downs, W. A. Snyder, W. J. Rhea, W. Chen, J. Fisher, W. P. Bissett, P. A. Reisse, "Ocean PHILLS hyperspectral imager: design, characterization and calibration," Opt. Express **10**, 210-221 (2002), http://www.opticsexpress.org/abstract.cfm?URI=OPEX-10-4-210
9. G. Baudin, R. Bessudo, M. A. Cutter, D. Lobb, J. L. Bezy: "Medium resolution imaging spectrometer (MERIS)," in *Future European and Japanese Remote-Sensing Sensors and Programs*, P. Slater Ed., SPIE vol. 1490, pp. 102-112 (1991)
10. http://www.semiconductor.agilent.com/spg/doc/diffract/htmlfiles/VS15.shtml
11. X. Wang, J. R. Leger and R. H. Rediker, "Rapid fabrication of diffractive optical elements by use of image-based excimer laser ablation," Appl. Opt. **36**, 4660-4665 (1997)
12. G. P. Behrmann and M. T. Duignan: "Excimer laser micromachining for rapid fabrication of diffractive optical elements," Appl. Opt. **36**, 4666-4674 (1977)
13. W. X. Yu, X. –C. Yuan, N. Q. Ngo, W. X. Que, W. C. Cheong and V. Koudriachov, "Single-step fabrication of continuous surface relief micro-optical elements in hybrid sol-gel glass by direct laser writing," Opt. Express **10**, 443-448 (2002), http://www.opticsexpress.org/abstract.cfm?URI=OPEX-10-10-443
14. P. Mouroulis, D. W. Wilson, P. D. Maker, and R. E. Muller, "Convex grating types for concentric imaging spectrometers," Appl. Opt. **37**, 7200-7208 (1998)

#2005 - $15.00 US Received January 06, 2003; Revised February 05, 2003

15. F. Scott, "The production of variable-transmission sinusoidal patterns and other images," Photogr. Sci. & Eng. **9**, 86 (1965)
16. P. Mouroulis, "Contrast sensitivity in the assessment of visual instruments," in *Assessment of Imaging Systems: Visible and Infrared*, T. L. Williams Ed., SPIE vol. 274, 202-210 (1981)
17. Center for Advanced Microstructures and Devices: http://www.camd.lsu.edu
18. Microchem Corporation, information on resists: http://www.microchem.com
19. Clariant Corporation, information on developer: http://www.azresist.com

1. Introduction

Grating fabrication techniques continue to evolve in response to new spectroscopic requirements and optical designs. A particular class of optical designs, concentric spectrometer forms, has been recognized for its potential for compact size and high performance [1-5]. There are two basic concentric spectrometer forms: the Offner spectrometer, requiring a convex grating, and the Dyson spectrometer, requiring a concave grating. Grating-based Offner spectrometers have already been in space missions [6,7] as well as airborne instruments [8,9], and there is even a laboratory instrument available as off-the-shelf item [10]. Several more similar instruments are at present under development in various laboratories around the world, including an instrument for NASA's Mars '05 orbiter.

The need to maintain a constant blaze angle along a curved surface comes in addition to the requirements for achieving a desired groove profile (efficiency), low scatter, and minimum ghosts, that are imposed on all gratings, curved or flat. The two mainstream techniques that have long existed for grating fabrication, ruling and holographic, cannot easily handle curved substrates. For ruled gratings, maintaining a constant blaze angle is problematic, as is maintaining coherence between panels in a multipanel grating. And of course, there is considerable scatter. Holographic techniques cannot easily generate a blazed profile on a curved surface, and have even greater difficulty handling shallow profiles (blaze angles less than a few degrees), frequently needed in low to medium resolution instruments. Laser writing and ablation techniques have also been reported [11-13], but the gratings thus produced seem to suffer from significant surface roughness [12, 13] or strongly nonlinear profile [13].

Gratings written through electron-beam (E-beam) lithography have been shown to present several critical advantages [14]. However, even that technique cannot satisfy all possible application requirements. One limitation arises from a maximum permissible sag of less than about 4 mm (depending on the E-beam writer). Another potential limitation for applications requiring extremely low parasitic light is the appearance of ghosts due to the periodicity of the writing pattern (field and sub-field stitching). We set out to develop an alternative technique, using X-ray lithography. Our motivation was the potential advantages that included absence of ghosts, low scatter, writing over a substrate of arbitrary shape as easily as on a flat substrate, ability to tailor the groove profile to any shape (not only sawtooth), and high wavefront quality.

In this paper we report on the techniques for grating fabrication using X-ray lithography and show results from the first test gratings produced on flat substrates. We also show the results from a depth-of-focus experiment that allow us to extrapolate the performance of gratings on curved substrates.

2. Summary of the method

The basic concept has been used in the past for coarse sinusoidal grating fabrication as well as non-periodic distributions using optical wavelengths on silver halide film [15,16]. A periodic area mask is generated that has a period equal to the desired grating period and a shape that depends on the desired groove (or transmittance) profile. The mask is then scanned at a constant speed across the photosensitive material (or the substrate translated across a stationary mask). The resulting motion creates a periodic pattern in which the exposure at any

#2005 - $15.00 US Received January 06, 2003; Revised February 05, 2003

point is proportional to the mask height along the direction of motion. Nonlinearities in the response of the photosensitive material can be accounted for by modifying the mask shape.

The first task then is to create an X-ray area mask with a linear profile. This serves either as a characterization mask, if the material response is non-linear, or directly as a final fabrication mask if the material responds linearly. We used two different masks, one for material and process characterization, and one for generating gratings. The first mask comprised three separated triangles as shown in Fig. 1(a). The second mask was periodic with a period (triangle height) of 20 μm and a base of 30 μm, shown in Fig. 1(b). The length of the base determines the maximum exposure.

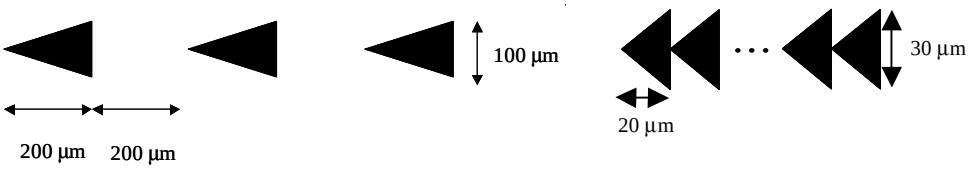

Fig. 1. (a) Schematic of the mask used for process characterization. The mask was used for stationary exposures of a fixed duration as well as for scanned exposures. The direction of the scan is vertical, along the base of the isosceles triangle. (b) Schematic of the mask used for generating gratings. The period is 20 μm and the base is 30 μm.

Once the mask has been fabricated, it is used to expose a substrate that is spin-coated with an appropriate photoresist. The exposures took place at the synchrotron maintained by the Center for Advanced Microstructures and Devices [17] of the Louisiana State University. The X-ray spectrum that is obtained at the beamline used is shown in Fig. 2.

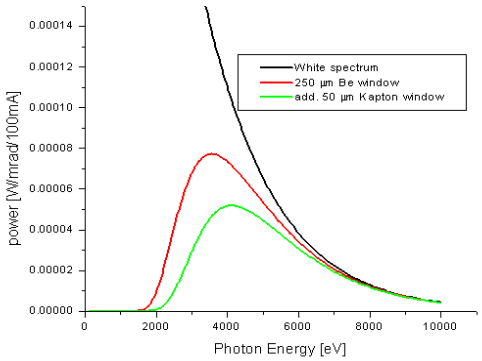

Fig 2. X-ray spectrum at the beamline. The green (lowest) curve represents the spectrum of the rays incident on the mask.

3. Choice of photoresist

This is the most critical aspect of the entire process. We experimented with three different resists, SU-8 (a chemically amplified, epoxy-based resist), PMMA (polymethyl-methacrylate) and PMGI (polymethylglutarimide), all from Microchem Corporation [18]. The last of the three was clearly the most successful, but we include in this section some comments about the other two.

#2005 - $15.00 US
Received January 06, 2003; Revised February 05, 2003

3.1 SU-8 resist

SU-8 is a negative resist (unexposed areas clear after development). The motivation for using it was its relatively high sensitivity to X-rays and correspondingly short exposure time. However, it also has a very high gamma, making it very difficult to obtain consistent gray scale. Extreme nonlinearity and poor repeatability were observed. Thus, although it was relatively straightforward to generate deep grooves, it was not possible to control the profile with sufficient accuracy. In order to generate blazed profiles with some repeatability it was found necessary to restrict the dynamic range of the exposure and work over a limited, essentially linear portion of the characteristic curve. This was achieved through a double exposure technique in which the resist was first given a uniform exposure to control the operating point, and then a spatially varying exposure that created the modulation. This effectively reduces the contrast produced by the triangular mask of Fig. 1(b). An equivalent method, but with less flexibility, would be to create a trapezoidal instead of triangular mask, which would contain the unmodulated as well as the modulated exposure simultaneously. However, it would be necessary to establish the proportions of the trapezoid through advance characterization.

The resist was processed and developed according to the manufacturer's recommendations (pre-bake and post-bake at 65 and 95^{o}C, develop in Microchem SU-8 developer). A blazed grating profile that was obtained with the double exposure technique is shown in Fig. 3. Although that appears to be a promising result, the overall difficulty of handling this resist led us to experiment with alternative ones in search of a more repeatable and well-behaved process. The main problems were 1) surface irregularity (a hint of which is shown in Fig. 3), and 2) extreme sensitivity of the grating profile to mask leakage (residual transmission through the gold), which is a consequence of the high sensitivity and nonlinearity of the process. This last problem exacerbated any small variations in mask absorption across its extent, to the point of creating significantly different profiles from one end to the other. The same mask created very good gratings with another resist, as shown in Section 5 below.

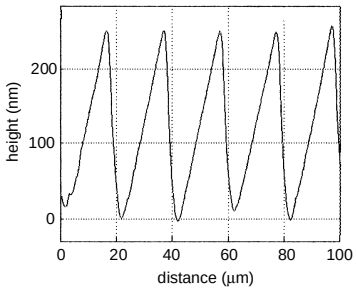

Fig. 3. Blazed grating profile generated on SU-8 resist.

3.2 PMMA resist

This resist provided more repeatable results but proved too slow for any but the shallowest of gratings. It also gave a nonlinear characteristic. We experimented with two methods of development, one using the recommended PMMA developer, and the second using pure acetone. Acetone development was ultimately preferable because it provided a considerably smoother surface for the same depth of removed resist. The resist was otherwise processed according to the manufacturer's recommendations (pre-bake at 180^{o}C for 90 s, no post-bake).

Some characteristic curves typical of those obtained are shown in Fig. 4. We used both stationary exposures, as well as scanned exposures (using the mask of Fig. 1(a)). In the first case, the exposure time is simply the dwell time, and in the second case, the exposure time is

#2005 - $15.00 US Received January 06, 2003; Revised February 05, 2003

calculated from the speed of the scan and the height of the triangle aperture at any one point. The two exposure methods gave similar results, with the scanned exposures showing slightly more depth (~10% on average). For clarity, we show only the stationary exposures in Fig. 4. The total exposure dose is measured in units of mA min, where the number of mA is the synchrotron beam current at the time of exposure (the same unit of ring current appears on the ordinate of Fig. 2). For comparison, typical dose for SU-8 resist was 0.1-0.3 mA min.

From Fig. 4, it can be seen that the response of the resist is nonlinear under all conditions of development. We may also note that although it was possible to obtain data after 20 s of development time with acetone, the resist coating was already damaged in several places. For a good quality surface, a maximum development time of 10 s would be recommended, thus reducing considerably the maximum depth. No gratings were fabricated with this resist.

3.3 PMGI resist

This resist gave the best results, and we provide characterization data in some detail. We experimented with different pre-bake temperatures that go well beyond the manufacturer's recommendations, since our use of the resist is very different from the one for which it was formulated. In general, it is found that increasing pre-bake temperature reduces the sensitivity of the resist. However, such hard-baked resist can withstand longer development time, so the same or more removed depth can be obtained after development. The manufacturer lists the glass transition temperature as 190°C, planarization temperature as 250-300°C and degradation temperature as 335°C. Normal recommended pre-bake temperature is 150-190°C. We used three temperatures, 170, 230, and 280°C. The resist was developed in AZ-300MIF developer from Clariant Corporation [19]. The maximum development time before resist degradation was found to be 4-5 min, 5-7 min, and 25-35 min for the three temperatures respectively.

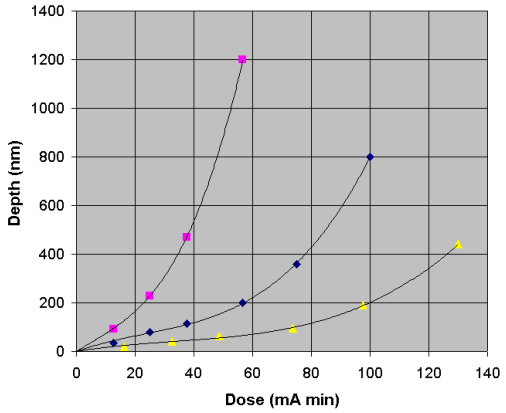

Fig. 4. Depth vs. dose characteristic of PMMA resist. Squares: developed for 20 s in acetone, diamonds: 10 s in acetone, triangles: 5 min in PMMA developer. Third degree interpolated polynomial curves are also shown.

An indication of the drastic resist sensitivity change with pre-bake temperature is given in Fig. 5. To obtain that figure, we recorded gratings using the mask of Fig. 1(b) and measured the modulation depth of the recorded grating. To make the comparison possible, we fixed the development time to 5 min. Although the pre-bake time differed between these three conditions (5 min for the first point and 30 min for the last two) it is thought that the temperature is much more significant than the time for such thin resist layers.

#2005 - $15.00 US Received January 06, 2003; Revised February 05, 2003

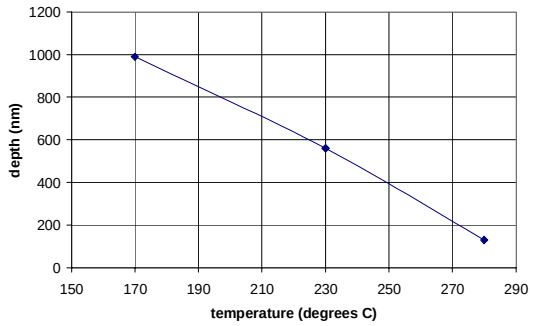

Fig. 5. Dependence of grating modulation depth on pre-bake temperature for PMGI resist.

To demonstrate the effect of development time on removed depth, we recorded gratings using two different masks with profiles similar to that of Fig. 1(b) but with some significant corner rounding (see also Fig. 10 below). The two masks gave the same developed modulation depth within reading error in all cases, so the average of the two was taken. Figure 6 shows the increase in modulation depth with development time. The resist was baked at 280°C. The same substrate was returned for further development after each measurement. The development was stopped after 55 min since it was obvious that the developer had attacked the resist. Other samples were attacked with less development time. Fortunately, signs of degradation are readily visible under a microscope; thus a cautious development procedure is possible whereby one can extract the maximum (or desired) depth from any sample by developing in small increments of time.

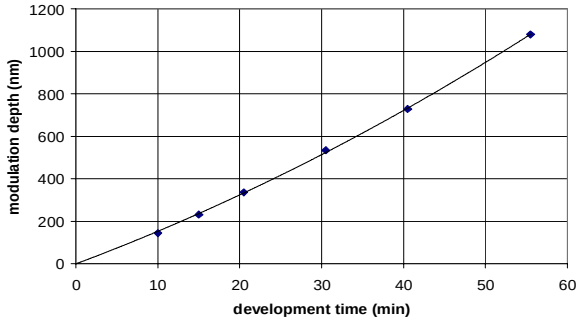

Fig. 6. Grating modulation depth vs. development time for PMGI resist (280°C pre-bake temperature), shown with a quadratic interpolated curve.

Significantly, the grating profile was practically unchanged through development, except of course for depth. Typical grating profiles are shown in Section 5.

The characteristic curves obtained with this resist are shown in Fig. 7 for a pre-bake temperature of 170°C and in Fig. 8 for a pre-bake temperature of 280°C. No further data were taken with the intermediate temperature of 230°C because, although the resist sensitivity is reduced, this temperature does not harden the resist sufficiently to withstand long development time.

#2005 - $15.00 US Received January 06, 2003; Revised February 05, 2003

It can be seen that the resist characteristic is perfectly linear at 170°C and slightly nonlinear at 280°C. However, the nonlinearity in the latter case would be observed only for deeper gratings, blazed in the infrared.

It should be clear that the removed resist is measured relative to the nearby unexposed area. However, even unexposed resist is affected by the developer. Thus the height of the unexposed but developed resist is less than the height of the originally deposited resist layer.

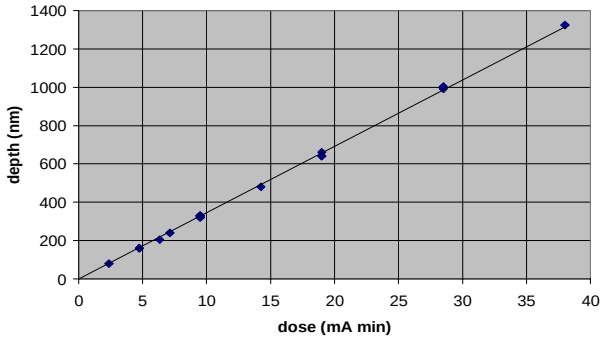

Fig. 7. Depth vs. dose for PMGI resist, 170°C pre-bake temperature. A linear interpolated curve is shown. The exact slope of the curve may vary somewhat from one sample to the next, but good linearity was observed on all samples.

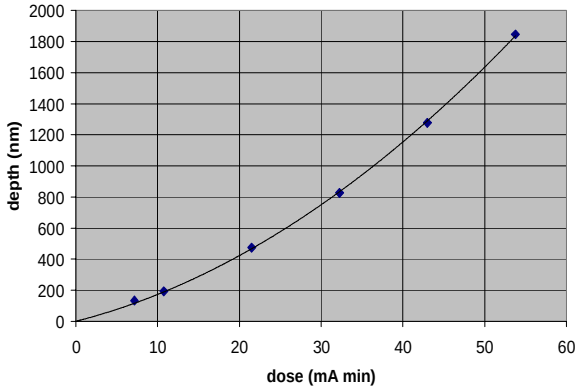

Fig. 8. Depth vs. dose for MPGI resist, 280°C pre-bake temperature. A quadratic interpolated curve is shown.

The linear and slightly nonlinear characteristics are also demonstrated clearly through the scanned images of the calibration (triangle) mask of Fig. 1(a). Stylus profilometer (Tencor P-2) scans of the corresponding images are shown in Fig. 9.

4. Mask fabrication

For our first attempt, a conventional mask fabrication method was employed. First, a chrome-on-glass negative mask with the desired pattern was generated through E-beam lithography. This was subsequently contact-printed onto a Si wafer coated with silicon nitride and a positive photoresist (Shipley 5740) using a Hg source at 410 nm. After development, the wafer was gold-plated to a height of between 5 and 10 μm. The remaining resist was

#2005 - $15.00 US Received January 06, 2003; Revised February 05, 2003

removed, and finally, the silicon was etched from the rear side to create a clear window with only the (gold-plated) nitride membrane. Thus the X-rays must be transmitted through only the nitride membrane (1-2 μm thick) and are blocked by a 5-10 μm thick layer of gold.

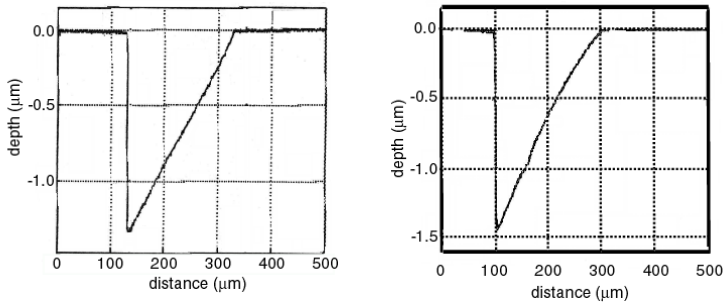

Fig. 9. Scanned image of one triangle from the mask of fig. 1(a). Left: 170°C, right: 280°C pre-bake temperature. Scan speed: 0.1 mm/min. Beam current: Left 38 mA, right: 42 mA.

X-ray images of the periodic masks generated in this fashion (corresponding to the pattern of Fig. 1(b)) are shown are shown in Fig. 10. Although different in the details, both masks demonstrate similar amount of rounding and thus created similar grating profiles. Most of the detail is lost during the contact print step through diffraction. The optical images of these masks looked similar to the X-ray imprints.

A more advanced mask fabrication technique is already under way and has shown promise of producing much sharper corners and leaving no gaps. A preliminary example is shown in Fig. 11. No gratings have yet been fabricated with these masks. Of course, diffraction during X-ray exposure will eventually degrade the corners and will provide the ultimate limit to the period as well as efficiency of these gratings.

Fig. 10. X-ray imprints of the two masks used to fabricate gratings. The period is 20 μm.

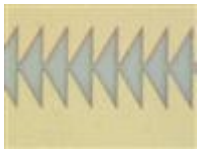

Fig. 11. Optical photograph of a mask made with improved technique. The period is 9 μm, Au layer thickness ~5 μm.

5. Grating test results

5.1 Efficiency

The gratings were fabricated on microscope slide substrates. To test their efficiency, a simple setup was constructed. The light from a monochromator slit was collimated and directed towards the grating. An aperture stop located near the grating limited the beam to the central ~1 cm diameter of the grating area. The angle of incidence was approximately 26°. The diffracted light was collected with a second lens and made to pass through a wide slit (~800

#2005 - $15.00 US Received January 06, 2003; Revised February 05, 2003

μm), about five times the size of the monochromator slit. A power meter with a large area detector collected all the light through the receiving slit, which was moved to track the shifting slit image as the wavelength changed. After this measurement, the microscope slide was translated sideways so that light was incident on an area where there was no grating, but had the same aluminum coating as the grating. The measurement was repeated again through wavelength. The grating efficiency was obtained as the ratio of the two measurements. Thus the quoted efficiency represents only the diffractive properties of the gratings and does not contain the reflectivity of the Al coating (relative efficiency). The repeatability of the measurement was ~1%.

Three gratings were tested, all with the same period. Two were made with a pre-bake temperature of 170°C and one with a pre-bake temperature of 280°C. They were also made with the two different X-ray masks of Fig. 10. The results are shown in Fig. 12.

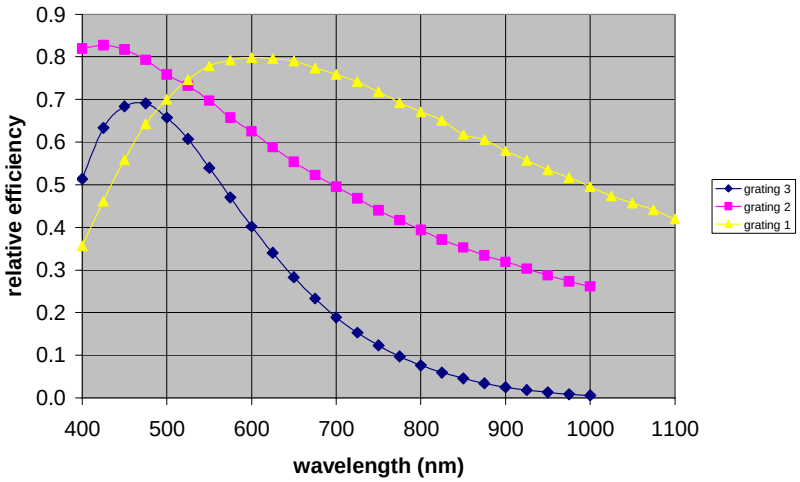

Fig. 12. Efficiency of three blazed gratings. For grating 1 and grating 2 (triangles and squares), the first order efficiency is shown, and for grating 3 (diamonds) the second-order efficiency.

A peak efficiency value between 80 and 82% is observed in the first order. This is consistent with the grating profiles obtained. A typical profile is shown in Fig. 13. All gratings made with these masks produced profiles almost identical with that of Fig. 13, the only difference being the depth of modulation (or blaze wavelength).

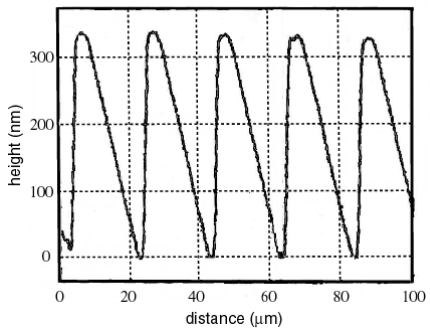

Fig. 13. Typical profilometer scan of gratings made with the masks of Fig. 10.

#2005 - $15.00 US
Received January 06, 2003; Revised February 05, 2003

5.2 Ghosts and scatter

Detailed characterization of these parameters will await a future experiment in which we will use gratings on curved substrates currently under fabrication. Here we provide some preliminary comments. A simple technique for evaluating ghosts is to use a charge injection device (CID) camera, which, unlike CCD cameras, suffers from no blooming artifacts independent of the level of saturation. This allows us to image the entire field between two orders, and increase the light level to the point where even weak ghosts become visible.

Through a combination of measurements with a photodetector and pictures taken with the camera, we can verify conservatively the absence of ghosts in the spectral direction at a level less than 10^{-5} (relative to the main order at 633 nm). This of course is not a surprising result since there are no periodic artifacts inherent in the fabrication process. In the perpendicular direction, which can be very important for imaging spectrometry applications, a ghost at a distance approximately equal to the distance between orders appeared. This is due to a periodic motion artifact produced by the feedback mechanism of the translation stage that has been observed in all scans and has a period of approximately 20 μm, accidentally similar to the grating period. This ghost is estimated to be around 10^{-4}, however we may note that it is not inherent in the process and would be eliminated with a better stage.

Scatter away from the main order, also called "grass", was not measured carefully but appeared to be very low, at a similar level as E-beam or holographic gratings. The groove quality shown in figure 14 would tend to support the absence of grass. However, one of the three gratings (grating 1), showed more parasitic light than the other two, especially in the direction perpendicular to the spectrum. This was likely due to stage motion problems, but we clearly have not yet produced a sufficient number of gratings for our results to be considered representative of the process, or to for us to fully understand the causes of variation. However, these preliminary results are certainly promising.

Finally, we should note that any mask imperfections such as holes in the coating will translate into grating imperfections. But that typically affects isolated grooves. Phase continuity is still preserved, even after a few bad grooves. In our masks there were only a few such defects over a length of 25 mm.

5.3 Effect of distance from mask

For this experiment, we fabricated seven gratings on a single substrate, at different distances from the mask. This way, all gratings received similar exposure and identical development. In addition, recording on a flat substrate facilitates the use of a profilometer for characterization.

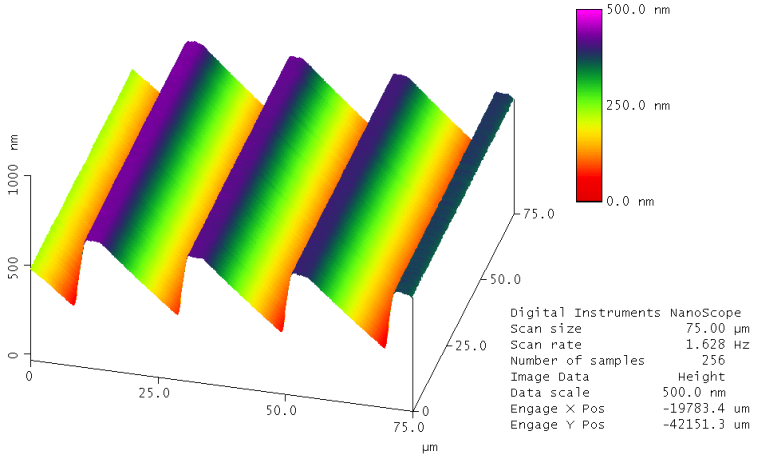

Fig. 14. Atomic force microscope scan of grating 3.

#2005 - $15.00 US Received January 06, 2003; Revised February 05, 2003

Of the seven gratings, the first one was recorded with the substrate as close as possible to the mask (est. <300 μm). For the remaining gratings, a translation stage was moved backwards in increments of 1.5 mm. The pre-bake temperature was 280°C and we took two scans of all the gratings, one after 15 min of development and another after 25 min. The results are plotted in Fig. 15. The scan speed was 0.1 mm/min for all cases. The differences in dose resulting from slightly different beam current were accounted for by normalizing the measured depth to the current of the first grating. However, that was a small correction (less than 6%).

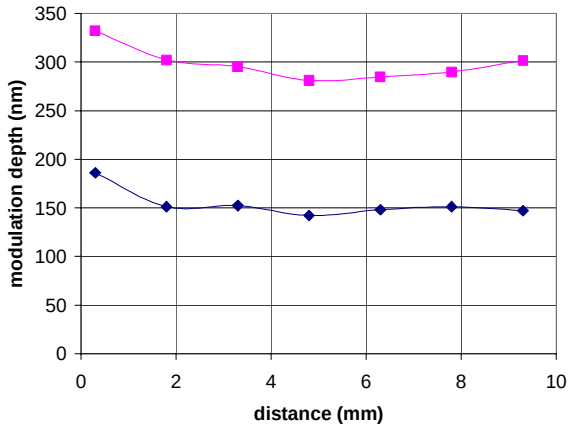

Fig. 15. Modulation depth of gratings as a function of distance from the mask for two different development times: 15 min (diamonds) and 25 min (squares).

It can be seen from Fig. 15 that the gratings give essentially constant modulation, independent of distance. There was also no visible difference to the profiles, which all looked like that of Fig 13. This result would allow the fabrication of curved gratings with a sag of several mm for this period. Interestingly, the first point in both curves of Fig. 15 is significantly higher than the rest. To confirm this result we repeated this experiment by writing four gratings at distances between 0 and 2 mm. Though not presented here, those results confirmed a small drop in modulation within the first 2 mm. However, although this may be an interesting effect to explain, a more important investigation will be to repeat these experiments with a sharper mask. In any case, even if we exclude the first 2 mm, this experiment shows that we can record a high-quality blazed grating with 20 μm period on a substrate with a sag of over 7 mm and of arbitrary (spherical or aspheric) shape. We believe that this is a significant result that cannot be easily duplicated by any other grating fabrication method. It is to be noted that concentric spectrometers even when operating at f/1, do not involve steeply curved surfaces, so the period is essentially constant across a curved grating.

6. Conclusions and outlook

We have presented our first results from a technique for fabricating blazed gratings on flat or curved substrates with substantial sag. High quality gratings can be generated. A relative peak efficiency of up to 82% has been demonstrated. Improvements in mask making techniques allow us to believe that the method is capable of even higher efficiency. [Note added in proof: 88% peak efficiency was demonstrated with improved masks]. The gratings present no inherent ghosts and can be made with smooth grooves.

It is important also to understand the limitations of the process. The width of the X-ray beam at our present beamline and location is about 8 cm and places a limit on the width of

#2005 - $15.00 US
Received January 06, 2003; Revised February 05, 2003

any grating. More important, however, is the resist sensitivity and resulting scan speed. The exposure time is determined by the scan speed and the base of the triangle mask. Thus, longer base length results in faster scan speed and/or larger grating area. But the base cannot be much more than about 3 times the period before mask alignment becomes critical; also the corners become more difficult to reproduce. The mask of Fig. 11 probably represents a practical limit in this respect. Multiple rows of masks can be used to increase the exposure while reducing the requirement for corner sharpness, but the rotational alignment would have to be quite accurate. In general, finer gratings will require lower scan speed, making the technique unsuitable for generating large, fine-pitch gratings. Fortunately, concentric spectrometer forms are preferred for their compactness and do not typically require large gratings. A practical limit to the grating pitch will come from the accuracy with which we can generate masks. Our aim is to demonstrate a 3 μm pitch with our present beamline. Below that size, harder X-rays may be needed to reduce diffraction.

The synchrotron is re-injected with electrons about three times a day. This sets a limit on the exposure time, although it would be possible in principle to stop the exposure and continue after injection. A small discontinuity or imperfection may result but it would be over a negligible area. However, the beam current varies substantially between injections sometimes by more than a factor of 2. In such a case, it would be necessary to alter the stage speed in real time to compensate for the beam current, something that we have not attempted to do so far. Finally, we note that all the gratings generated to date have been exposed with a beam current of about 40 mA, which is rather low. The synchrotron is capable of over three times that current. Such high current would reduce the exposure time and/or allow larger gratings.

Acknowledgments

We are indebted to the CAMD staff (Jost Gottert, Zhong-Geng Ling, Tracy Morris, Shaloma Malveaux and Lorraine Day) for assistance in setting up the beamline, and technical and safety training and support. This research has been partly performed at the Jet Propulsion Laboratory, California Institute of Technology, under a contract with the National Aeronautics and Space Administration. Funding was provided under a NASA Cross-Enterprise Technology Development Grant.

#2005 - $15.00 US Received January 06, 2003; Revised February 05, 2003